Hydrodynamic Interactions in Concentrated Suspensions

X. Qiu,[1,2] X. L. Wu,[1,3] J. Z. Xue,[1,3] D. J. Pine,[1] D. A. Weitz,[1] and P. M. Chaikin[1,3]
[1]*Exxon Research and Engineering Company, Route 22 East, Annandale, New Jersey 08801*
[2]*Department of Physics, University of Pennsylvania, Philadelphia, Pennsylvania 19104*
[3]*Department of Physics, Princeton University, Princeton, New Jersey 08540*
(Received 9 March 1990)

We study the effects of hydrodynamic interactions on the diffusion of hard spheres in concentrated suspensions. Using a multiple-light-scattering technique that measures the early-time behavior, we find $D_{\rm eff}/D_0 = 1 - (1.86 \pm 0.07)\phi$, where ϕ is the volume fraction of spheres, $D_{\rm eff}$ is the effective diffusion coefficient, and D_0 is the free-particle diffusion coefficient. This agrees with the linear ϕ term calculated theoretically for short-time self-diffusion. The short-time diffusion coefficient is also found to be continuous across the freezing transition.

PACS numbers: 82.70.Kj, 66.90.+r, 82.70.Dd

A system of spheres interacting only through their inability to occupy the same space has served as a paradigm for our understanding of the structure and dynamics of liquids, solids, and glasses. Suspensions of these "hard spheres" have likewise served as a paradigm for the calculation of hydrodynamic interactions between colloidal particles. As the volume fraction of suspended particles is increased, simple single-sphere hydrodynamic theories for the transport coefficients fail and many-sphere hydrodynamic interactions become important. Potential interactions, such as the excluded-volume hard-sphere interaction, indirectly influence the kinetics and mobility of the suspension through their effects on the equilibrium thermodynamics and structure. By contrast, velocity-dependent hydrodynamic interactions directly affect the kinetics and mobility and play no role in the thermodynamics and structure. The hydrodynamic interactions in concentrated suspensions are traditionally the hardest to determine theoretically and experimentally and are the primary subject of this paper.

One of the most direct probes of hydrodynamic interactions is the short-time self-diffusion coefficient of a tagged sphere. For times much less than the time it takes a particle to diffuse the mean interparticle separation, a tagged sphere does not contact other spheres and the potential interactions between spheres are negligible; only the hydrodynamic interactions play a role. At longer times, however, the motion of a sphere is impeded by collisions with other particles which it must "get around" and then the self-diffusion involves a combination of structural and hydrodynamic effects. Thus, hydrodynamic interactions are probed most directly in the short-time regime.

Hydrodynamic interactions also play a crucial role in the collective diffusion of colloidal particles. Consider a concentration fluctuation of wave vector q. The susceptibility of the system to such a fluctuation is directly related to $S(q)$, the static structure factor. The relaxation of the system back to uniform equilibrium will be inversely proportional to $S(q)$.[1] Relaxation of the fluctuation does not require particles to "get around" neighbors but particle motion is still impeded by mutual hydrodynamic interactions. Thus, the cooperative diffusion coefficient, which is a measure of relaxation of spontaneous fluctuations, is affected by both potential and hydrodynamic interactions. However, at short times, the effect of the potential interactions for hard-sphere systems can be accounted for trivially through $S(q)$.[1,2] Once again the *short-time* dynamical behavior can be used to probe the hydrodynamic interactions between spheres.

For concentrated hard-sphere systems, the collective-diffusion coefficient $D_c(q)$ exhibits a strong q dependence. For $qR \ll 1$, where R is the particle radius, the hard-core repulsive potential leads to fast initial relaxation and a relatively large value of $D_c(q)$. For $qR \gg 1$, the relaxation of concentration fluctuations is determined primarily by single-particle motions and $D_c(q)$ should approach the short-time self-diffusion coefficient measured in tracer experiments.

To measure short-time particle diffusion we employ a dynamic light-scattering technique, diffusing wave spectroscopy (DWS), in the transmission mode.[3] In DWS, the temporal fluctuations of *multiply scattered* light are analyzed to obtain particle-diffusion coefficients.[3-6] By utilizing the transmission mode, particle motion is probed over significantly shorter time and length scales than is possible with either traditional single-scattering techniques or other multiple-scattering geometries. Because light scatters from concentration fluctuations, the fundamental quantity DWS measures is the collective-diffusion coefficient $D_c(q)$. However, since the light is scattered many times, all scattering angles are probed simultaneously, and $D_c(q)$ is effectively averaged over a wide range of q. As we show below, this averaging strongly weights the high-q limit so that the diffusion coefficient measured by DWS approaches the self-diffusion coefficient. Thus, using two sets of particle sizes, we measure an effective diffusion coefficient $D_{\rm eff}$

 © 1990 The American Physical Society

and find that, to first order in the volume fraction of spheres ϕ, it is well described by

$$D_{\text{eff}}/D_0 = 1 - (1.86 \pm 0.07)\phi , \quad (1)$$

for $0.03 < \phi < 0.45$. The coefficient of the linear term is in excellent agreement with calculations of the self-diffusion coefficient by Batchelor[7] who found 1.83ϕ. When compared with tracer-diffusion measurements of van Megan *et al.*,[8] these measurements also indicate that the hydrodynamic corrections to the early-time self- and cooperative-diffusion coefficients are the same.

The samples used in our studies were aqueous suspensions of polystyrene spheres (polyballs) purchased commercially. Polyballs are often used as a model "soft-sphere" suspension since they are negatively charged in suspension and interact via a screened Coulomb repulsion. However, the screening length is inversely proportional to the square root of the density of ions in the electrolyte solvent and is easily controlled. The polyballs used here were cleaned by ion-exchange resins and then sufficient HCl was added to reduce the screening length to ~ 40 Å. The diameters of the spheres, as measured by dynamic light scattering (DLS) on very dilute solutions, were 0.412 and 0.913 μm. Thus, the screening length was considerably smaller than the particle diameter and resulted in less than a 2% correction to the hard-sphere approximation, which is less than the polydispersity of the spheres ($\sim 5\%$).

Stock suspensions of concentrated monodisperse polyballs were prepared by first centrifuging to $\phi \simeq 0.55$. (Near 0.50 the suspension was in the crystalline state as readily observed by the Bragg scattering of visible light.) Portions of the stock suspensions were then diluted to prepare a series of samples having volume fractions ranging from 0.03 to 0.55. The volume fractions were determined to within ± 0.005 by weighing a fraction of each sample before and after drying.

Concentrated suspensions of polyballs whose diameters are comparable to the wavelength of light are typically white and opaque. As such, they are not suitable for conventional DLS studies. However, they are ideally suited for DWS which can be used only in the limit of very strong multiple light scattering. In the transmission geometry which we employ, DWS has the additional advantage that only the short-time diffusion of the suspended particles is measured. In DWS, as in DLS, an appreciable decay in the measured temporal autocorrelation function of the scattered light occurs when the path length of scattered photons from a given sequence of particles changes by roughly one wavelength. In an optically thick sample, each photon must be scattered many times (typically 10^2 to 10^4) before being detected; the difference in path length then results from the sum of displacements of a large number of particles. Thus, the movement of a typical particle is much less than the wavelength of light. In our measurements, a typical particle is estimated to move less than 50 Å before the autocorrelation function decays. This distance is much less than the mean interparticle spacing so that we always measure the short-time diffusion of the polyballs.

In our measurements, a laser beam ($\lambda_0 = 488$ nm) was expanded and collimated to uniformly illuminate a 1-cm-diam spot on one side of a cuvette containing the polyball suspension. The light emerging from the opposite side was detected by a photomultiplier, and the static intensity and temporal autocorrelation function were measured by a correlator. The thickness of the sample cell was varied from 0.2 to 2 mm for samples having different volume fractions. The ratio of the sample thickness to transport mean free path, L/l^*, ranged from 12 to 35 ensuring multiple scattering.

In the single-scattering case, light is scattered by concentration fluctuations and DLS measures the cooperative diffusion of polyballs.[9] The cooperative-diffusion coefficient $D_c(q)$ is given by the bare Stokes-Einstein diffusion coefficient D_0 renormalized by the susceptibility, as given by the static structure factor $S(q)$,[1,2] and by the hydrodynamic interactions via a factor $H(q)$:[10]

$$D_c(q) = D_0[H(q)/S(q)] . \quad (2)$$

Thus, in the short-time limit, the decay of the electric-field autocorrelation function in DLS is given by

$$\langle E(0)E^*(\tau)\rangle \simeq S(q)\exp\{-q^2 D_0 \tau H(q)/S(q)\} . \quad (3)$$

We can view the multiple-scattering process in an interacting system as a succession of isolated scattering events from correlated regions of spatial extent ξ and separated by the photon mean free path l where, in general, $\xi < l$.[4,5,11] For a large number of scattering events, n, the contribution to the decay of the autocorrelation function from paths of length $s = nl$ is given by the product of the single-scattering autocorrelation functions, averaged over all angles, $\exp\{-\langle q^2 D_0 \tau H(q)/S(q)\rangle n\}$, where $\langle \cdots \rangle$ denotes the angular average weighted by the product of the particle form factor and the structure factor, $F(q)S(q)$.[5] To facilitate the calculation, we express the number of scattering events, $n = s/l = (s/l^*) \times (l^*/l)$, in terms of the transport mean free path l^*, which is given by[12]

$$\frac{l^*}{l} = \frac{2k_0^2 \int F(q)S(q)\,d\Omega}{\int q^2 F(q)S(q)\,d\Omega} , \quad (4)$$

where $d\Omega$ is the solid angle element, $k_0 = 2\pi/\lambda$, and λ is the wavelength of light in the medium. The total autocorrelation function, $g_1(\tau) \equiv \langle E(0)E^*(\tau)\rangle / \langle |E(0)|^2 \rangle$, is obtained by summing the contributions of paths of all lengths, weighted by $P(s)$, the fraction of paths of length s (determined by the geometry of the sample and the optics). Performing the appropriate averages yields

$$g_1(\tau) = \int P(s)\exp\left\{-2k_0^2 D_0 \tau \frac{[H(q)]}{[S(q)]} \frac{s}{l^*}\right\} ds , \quad (5)$$

where $[\cdots]$ denotes

$$[X(q)] = \frac{\int X(q)F(q)q^2 d\Omega}{\int F(q)q^2 d\Omega}. \quad (6)$$

The only length scale entering Eq. (5) for the transport of photons is l^*, the length scale over which the direction of photon propagation is randomized. Thus, the photon path-length distribution function $P(s)$ can be calculated for a given scattering geometry using the diffusion equation for photons with appropriate boundary conditions.[5,13] It can be shown that for forward scattering with a broad illumination the autocorrelation function is[5]

$$g_1(\tau) = \frac{(L/l^* + \frac{4}{3})\sqrt{x}}{(1+\frac{4}{9}x)\sinh(L\sqrt{x}/l^*) + \frac{4}{3}\sqrt{x}\cosh(L\sqrt{x}/l^*)}, \quad (7)$$

where $x = 6k_0^2 D_0 \tau [H(q)]/[S(q)] \equiv 6\tau/\tau_0$. From Eq. (7) we see that one effect of multiple scattering is to speed up the decay of the autocorrelation function by a factor of $\sim(L/l^*)^2$. In addition, the diffusion coefficient is again modified by $H(q)/S(q)$, as in the single-scattering limit, but now suitably averaged over all scattering angles because of multiple scattering.

In our experiment we measure intensity-intensity autocorrelation functions $\langle I(\tau)I(0)\rangle/\langle I(0)\rangle^2 = 1+\beta g_2(\tau)$, where β is a constant determined primarily by the collection optics and $g_2(\tau)$ is related to $g_1(\tau)$ by $g_2(\tau) = |g_1(\tau)|^2$.

In Fig. 1 we plot the logarithm of the measured intensity autocorrelation function, $g_2(\tau)$, for the 0.913-μm spheres versus normalized time $(L/l^*)^2\tau$. The rate of decay of $g_2(\tau)$ in these normalized-time units depends only on the motion of the polyballs, and is independent of L/l^*. The three curves are for volume fractions of 0.08, 0.26, and 0.47. The autocorrelation function decays more slowly for the more concentrated samples indicating a large reduction in the diffusion coefficient from the free-diffusion value. Similar behavior is found for 0.412-μm diam spheres. The solid lines in Fig. 1 are fits by Eq. (7) with τ_0 as the only adjustable parameter. The fact that the functional form fits the data precisely indicates that there is no additional time dependence to be found in Eq. (7) and that we are in the short-time limit where the particle dynamics are purely diffusive. This is equivalent to obtaining a single slope in the logarithm of the correlation function versus time for a DLS experiment, indicating a single relaxation time. For the $\phi = 0.47$ sample shown in Fig. 1, the total motion of a particle in the decay time is ~ 50 Å.

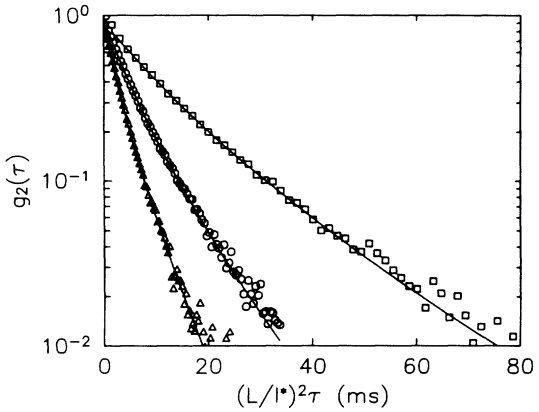

FIG. 1. Autocorrelation function vs normalized time. The measurements are for 0.913-μm-diam polyballs at volume fractions of 0.08 (triangles), 0.26 (circles), and 0.47 (squares), respectively. The solid lines are the fits by Eq. (7).

In order to elucidate the specific role of the hydrodynamic interactions we analyze these experimental data by defining an effective diffusion coefficient which retains only the q-independent, short-range hydrodynamic effects,

$$D_{\text{eff}} = D_0 H(\infty). \quad (8)$$

This effective diffusion coefficient should be the same as the short-time self-diffusion coefficient measured in tracer experiments.[8] We obtain D_{eff} by multiplying the fitting parameter τ_0^{-1}, obtained from our measurements of $g_2(\tau)$, by fk_0^2, where f is a numerical factor, $f \equiv [S(q)]H(\infty)/[H(q)]$. To compute these averages, we use the Percus-Yevick[14] form of $S(q)$, the Beenakker-Mazur[15] form of $[H(q)]/H(\infty)$ for hard spheres, and perform the angular averages numerically.[16] The angular average in Eq. (6) corresponds to a $q^3F(q)$ weighting over the interval from 0 to $2k_0R$, and strongly emphasizes the high-q limit where f approaches 1. For hard spheres, the peak in $S(q)$ occurs at $qR \approx 3$; in our experiments, $2k_0R = 7.1$ for 0.412-μm-diam spheres and $2k_0R = 16$ for 0.913-μm-diam spheres. Thus, in DWS experiments on large spheres, f will be close to 1 and only a weak function of ϕ. In our experiments, $0.78 < f < 1.0$ for the 0.412-μm-diam particles and $0.92 < f < 1.0$ for the 0.913-μm-diam particles for $0 < \phi \leq 0.45$. We calculate l^* using the Mie scattering formulas for the form factor $F(q)$ and again use the Percus-Yevick form for $S(q)$.[12] The ratio L/l^* is also measured experimentally by the transmission intensity of each sample and is in good agreement with the calculations, but has larger error bars.

The effective diffusion coefficient D_{eff}, normalized by the Stokes value D_0 $(= k_BT/6\pi\eta R)$, is plotted versus volume fraction in Fig. 2 for all of our samples. We have also plotted the short-time self-diffusion coefficient from a tracer measurement reported by van Megan *et al.*[8] The data sets are indistinguishable at low volume fractions and are only slightly different at higher volume fractions. This difference is probably due to the uncertainties in the theoretical values of $H(q)/H(\infty)$ required

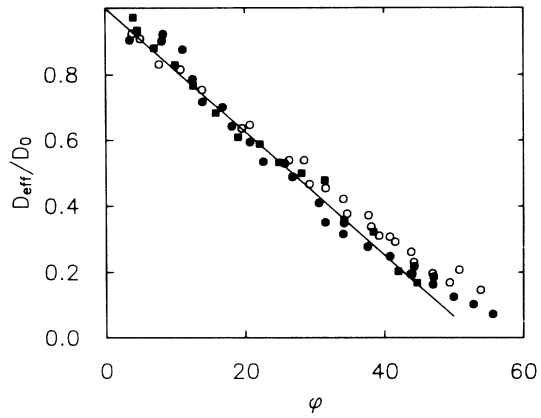

FIG. 2. Normalized effective diffusion coefficient vs volume fraction. The solid squares and circles indicate the 0.412- and 0.913-μm-diam particles, respectively. The solid line is the theoretical fit using Eq. (1). The open circles are short-time self-diffusion coefficients measured by van Megan *et al.* (Ref. 8).

to interpret our data. These uncertainties are most pronounced at high volume fractions. Nevertheless, to within the scatter of our data, the hydrodynamic corrections to the short-time self- and cooperative-diffusion coefficients appear to be the same. Our data can be fitted reasonably well by the linear form in Eq. (1). There have been many attempts to calculate the coefficient of the linear ϕ term over the past several decades. Only the most recent calculations[7] obtain the value 1.83, which is in excellent agreement with our results.

Finally, we note that $D_{\rm eff}$ varies smoothly as the liquid-solid transition is crossed at $\phi=0.50$. The structure factor used to calculate $D_{\rm eff}$ for these samples is the Percus-Yevick form rather than the actual set of Bragg peaks for the crystalline phase. Nevertheless, the continuity of the data across $\phi=0.50$ illustrates the short-time nature of our measurement. The particles in the crystal move diffusively on a short time scale and only at longer times feel the strong potential of the surrounding cage of particles which traps them in a single cell of the solid.

In conclusion, we have used DWS to measure the effect of hydrodynamic interactions on the cooperative diffusion of concentrated hard-sphere systems. In contrast to previous DLS tracer experiments, these DWS transmission measurements provide an unambiguous determination of the short-time diffusion coefficient, allowing the effects of hydrodynamic interactions to be probed directly. The corrections from the average structure factor to f confirm that DWS measures cooperative diffusion. The agreement of the hydrodynamic corrections to both cooperative and self-diffusion comes largely from the fact that our measurements probe the intermediate- to high-q regime. These experiments clearly establish the weighting inherent in the quantities measured by DWS, and make possible detailed comparison with theoretical calculations.

[1]B. J. Ackerson, J. Chem. Phys. **64**, 242 (1976).

[2]P. N. Pusey and R. J. A. Tough, J. Phys. Math. Gen. **15**, 1291 (1982).

[3]D. J. Pine, D. A. Weitz, P. M. Chaikin, and E. Herbolzheimer, Phys. Rev. Lett. **60**, 1134 (1988).

[4]G. Maret and P. E. Wolf, Z. Phys. B **65**, 409 (1987).

[5]D. J. Pine, D. A. Weitz, G. Maret, P. E. Wolf, E. Herbolzheimer, and P. M. Chaikin, in *Scattering and Localization of Classical Waves in Random Media,* edited by P. Sheng (World Scientific, Singapore, 1990).

[6]P. E. Wolf and G. Maret, in *Scattering in Volumes and Surfaces,* edited by M. Nieto-Vesperinas and J. C. Dainty (Elsevier, Amsterdam, 1990).

[7]G. K. Batchelor, J. Fluid Mech. **74**, 1 (1976); **131**, 155 (1983).

[8]W. van Megan, S. M. Underwood, R. H. Ottewill, N. St. J. Williams, and P. N. Pusey, Faraday Discuss. Chem. Soc. **83**, 47 (1987).

[9]P. N. Pusey, J. Phys. Math. Gen. **8**, 1433 (1975).

[10]I. Snook, W. van Megan, and R. J. A. Tough, J. Chem. Phys. **78**, 5825 (1983).

[11]F. C. Mackintosh and S. John, Phys. Rev. B **40**, 2383 (1989).

[12]P. E. Wolf, G. Maret, E. Akkermans, and R. Maynard, J. Phys. (Paris) **49**, 63 (1988).

[13]A. Ishimaru, *Wave Propagation and Scattering in Random Media* (Academic, New York, 1978).

[14]W. Hess and R. Klein, Adv. Phys. **32**, 173 (1983).

[15]C. W. J. Beenakker and P. Mazur, Physica (Amsterdam) **126A**, 349 (1984).

[16]We emphasize that we only use the *wave-vector* dependence of $[H(q)]/H(\infty)$ calculated by Beenakker and Mazur, and not their values of $H(\infty)$, which disagree with the more rigorous low-ϕ theory (Ref. 7). Since we perform a q average over $H(q)$, and since the effects of $[H(q)]$ tend to counteract those of $[S(q)]$, our results are insensitive to the exact form of $H(q)$. Thus, to within experimental uncertainty, our results are unchanged when we use the calculation of Snook, van Megan, and Tough (Ref. 10) for $H(q)/H(\infty)$.